Numerical Analysis and Parametric Optimisation of Heat Release from a Packed Bed ($MgSO_4$) Thermochemical Reactor

Swaraj Kumar B, James Varghese, Aboobacker Kadengal

Abstract: ***Thermochemical energy storage is one of the process which is capable of both short term and long term energy storage. Incorporating this storage method with solar energy is important when we considering seasonal or long term thermal energy storage. Thermochemical energy storage uses chemical reactions to store and release the energy. The charging or storage temperature of the thermochemical material (TCM), porosity of the reactor bed, concentration of reactants etc. are some of the important factors which affects the storage and release of the energy of a TCM. In this work we investigate the energy release from $MgSO_4$ by modelling the hydration reaction of $MgSO_4$ in a packed bed reactor with continuous flow of moist air through the bed. It is observed that the parameters such as porosity of the reactor bed, mass flow rate of moist air, particle diameter, concentration of water vapour etc. play an important role on the energy release from the TCM. Thaguchi method is used to optimize these parameters. The porosity of the reactor bed and the particle size of the TCM are found to be crucial in energy release.***

Keywords **: *Thermal energy storage, Adsorption Kinetics, thermo-chemical material, Packed bed reactor, $MgSO_4$***

I. INTRODUCTION

All conventional energy sources in the world are in a depleting mode and the depletion rate is alarmingly fast. This trend will increase the energy cost [2] in very near future. But the energy demand is always increasing and the consumption of energy is in an all time high. Increasing energy consumption from conventional sources affects the environment as atmospheric pollution and climate change [3]. One solution for exploiting mother earth in this manner is to adopt the advanced, efficient and clean energy technologies for different applications [4-6] which will help to reduce the use of conventional energy sources. Waste energy recovery, use of renewable energy sources, suitable energy storage methods are some of the technologies used worldwide [7-10]. All these methods will help to reduce the use of conventional energy and bridge the gap between the energy supply and demand.

Revised Manuscript Received on January 15, 2020

***** Correspondence Author

Swaraj Kumar B*, Dept. of Mechanical Engg., LBS College of Engg. Kasaragod

Dr. James Varghese, Division of Mechanical Engg., CUSAT

Dr. Aboobacker Kadengal, Dept. of Mechanical Engg., LBS College of Engg. Kasaragod

Different thermal energy storage (TES) systems [11-15] store the excess energy and supply this stored energy during the peak demand. So thermal energy storage technologies are viable solutions for maintaining a balance between energy supply and demand. Many factors affect the selection of appropriate TES technology, some of them are storage time, temperature requirements, storage capacity, heat losses etc. Among the commonly used TES systems i.e., Sensible, Latent and chemical, Thermochemical energy storage (TCES) systems have increased attention of researchers recently. In TCES energy is stored by a dissociation reaction and recovered it in a reversible reaction. Thermochemical energy storage has high storage density than the other TES systems which allows large amount of energy to be stored in small amount of storage material, which also helps to reduce the overall size of the storage system. TCES is more suitable for long term energy storage or seasonal storage of energy because of no heat loss during the storage period and the storage can be done at ambient temperature.

There are a number of reacting pairs for thermochemical energy storage, but to incorporate the storage system with solar energy the working temperatures should not be very high. So, the selection of thermochemical material (TCM) is also important in TCES. The requirements for good TCM are high energy density, low reaction temperature, non-toxic, non-corrosive etc. [5]. Considering these requirements $MgSO_4$ / H_2O pair is a promising candidate for TCES. The charging temperature of the $MgSO_4 7H_2O$ ranging from 50^oC to 275^oC which can be achieved by a solar collector [12,13].

The objective of the present study is to investigate the suitability of $MgSO_4$ as a thermochemical storage material by using a finite volume method of analysis for its hydration reaction in a packed bed reactor and to optimize the parameters which affects the performance of the TCES system using Thaguchi method. Effect of porosity of the packed bed, pressure drop across the reactor vessel, particle diameter of the salt, concentration of water vapor at inlet, and heat capacity of the reactor wall on thermal dynamics in terms of adsorption-desorption reaction and temperature profile at the outlet of the reactor with time are analyzed**.**rectification in the final paper but after the final submission to the journal, rectification is not possible.

II. MATHEMATICAL MODELLING

A. Adsorption kinetics

The attraction between adsorbate molecules and adsorbent surface involve molecular forces otherwise known as Van Der Waal's forces. This physical adsorption is characterized by the liberation of heat [19]. In this study moist air at ambient temperature is modelled to flow through a porous bed of dry $MgSO_4$, the water vapour in the moist air absorbed by the dry $MgSO_4$, liberating heat to the surroundings. Thus the air at the outlet will be of higher temperature and lower relative humidity than the inlet condition. The problem domain is shown in Fig 1.

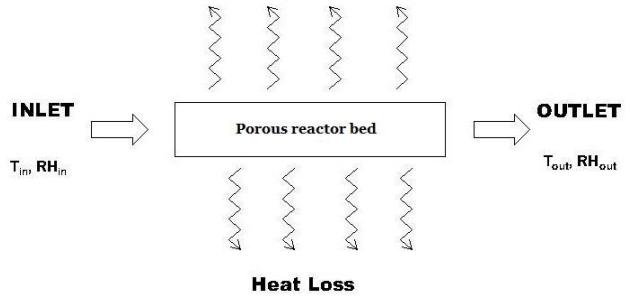

Fig.1 Simulated domain

The chemical reaction of this process is shown below.

$$MgSO_4 + 7H_2O \rightarrow MgSO_4 7H_2O + \Delta H$$

Where ΔH is the heat liberated during the reaction. From the chemical reaction, it can be seen that one mole of $MgSO_4$ adsorbs 7 moles of H_2O to form one mole of $MgSO_4.7\ H_2O$ and liberate 100 kJ of heat. Using this data, the maximum number of moles of H_2O that can be absorbed by 1 kg of $MgSO_4$ is calculated. When the vapor comes in contact with the salt, the amount of vapor adsorbed, 'q' is always less than the maximum possible. It depends on the partial pressure of the water vapor and the temperature. The adsorption kinetics of the system is represented by the linear driving force (LDF) approximation

$$\frac{dq}{dt} = k_m(q_{eq} - q) \tag{1}$$

Where 'q' and 'q_{eq}' are the originally absorbed and equilibrium mole of water by dry $MgSO_4$ and 'k_m' is the mass transfer coefficient.

The equilibrium loading of water on $MgSO_4$ is estimated by Langmuir isotherm

$$q_{eq} = q_{max}\frac{bp}{1+bp} \tag{2}$$

Where 'p' is the partial pressure of the vapour and 'b' is given by the following equation.

$$b = Ae^{(-\Delta H/RT)} \tag{3}$$

'A' is the Arrhenius factor for the chemical reaction, 'R' is the universal gas constant, T is the temperature, and 'ΔH' is the heat of adsorption.

The mass transfer coefficient 'k_m' is given by

$$k_m = \left(\frac{d_p}{6k_f} + \frac{d_p^2}{60\ \epsilon_b\ D_p}\right) \tag{4}$$

Where d_p is the particle diameter, k_f is the mass transfer coefficient for the fluid film around the particle, ϵ_b is the porosity and D_p is the macro pore diffusivity.

The process involving adsorption or evaporation the mass balance should include an axial dispersion term in terms of Sherwood number [21]. It was shown that the mass transfer coefficient could be expressed in terms of the dimensionless Sherwood number (Sh) by the relation

$$Sh = \frac{k_f D_p}{D_m} = 2 + 1.1Sc^{0.33}Re^{0.6} \tag{5}$$

Where 'Sc' is Schmidt number, Re is Reynold's number and D_m is the molecular diffusivity. The macro pore diffusivity D_p is a lumped parameter consisting of tortuosity factor (τ), molecular diffusivity (D_m) and Knudsen diffusivity (D_k).

In pores of diameter much greater than the mean free path of a molecule, diffusion occurs by a process of molecular collisions in the gas phase within the pore (called Maxwell or bulk diffusion), if the molecular mean free path is much greater than the pore diameter, diffusion occurs by molecules colliding with the pore walls (Knudsen diffusion).

$$D_p = \frac{1}{\tau}\left(\frac{1}{D_m} + \frac{1}{D_k}\right)^{-1} \tag{6}$$

B. Assumptions

- The flow in the reactor can be described by an axially dispersed plug flow model.
- radial gradients in the bed are negligible; therefore, heat and mass transfer balances are considered as one-dimensional problems.
- the gas phase behaves as an ideal gas and is in thermal equilibrium with solid phase
- the adsorbent particles have identical characterizations and the bed properties are uniform.

Based on these assumptions, the governing heat and mass balance can be written by a set of partial differential equations with space coordinate *z*, and time coordinate *t*.

C. Governing equations

Water mass balance equation

$$\frac{\partial c}{\partial t} + u\frac{\partial c}{\partial z} - D_z\frac{\partial^2 c}{\partial z^2} + \frac{(1-\epsilon_b)}{\epsilon_b}\rho_p\frac{dq}{dt} = 0 \tag{7}$$

where, c is the water vapor concentration, ϵ_b is the bed

porosity, ρ_p is the particle density of the salt, q is the average amount of adsorbed water per kg of salt, u is the velocity of flow and D_z is the axial dispersion coefficient. This coefficient is derived from Wakao's relation,

$$\frac{\epsilon_b D_z}{D_m} = 20 + 0.5ReSc \quad (8)$$

where D_m is the molecular diffusivity, Re is the Reynolds number ($\frac{\rho_g \epsilon_b u d_p}{\mu_g}$), Sc is the Schmidt number ($\frac{\mu_g}{\rho_g D_m}$) and μ_g is the viscosity of the feed gas.

2.3.1 Energy balance

$$\rho C_p \frac{\partial T}{\partial t} + \epsilon_b \rho_g C_{p,g} u \frac{\partial T}{\partial z} - k_{eff} \frac{\partial^2 T}{\partial z^2} - (1-\epsilon_b)\rho_p \frac{dq}{dt}\Delta H + \frac{4h_i}{d_i}(T - T_{wall}) = 0 \quad (9)$$

In the above equation, T is the temperature of the gas, $C_{p,g}$ is the specific heat capacity of the gas, h_i is the heat transfer coefficient of porous medium to the reactor wall, d_i is the

$$\rho C_p = \epsilon_b \rho_g C_{p,g} + (1-\epsilon_b)\rho_p C_{p,s} + (1-\epsilon_b)\rho_p q C_{p,water} M_{water} \quad (10)$$

inner diameter of the reactor and T_{wall} is the wall temperature.

The overall volumetric heat capacity ρC_p is given by the following equation:

The overall volumetric heat capacity consists of the heat capacity of the air in bed voids, the heat capacity of the air in pores, the heat capacity of the solid and the heat capacity of the adsorbed water.

Here, $C_{p,s}$ is the specific heat capacity of the salt, $C_{p,water}$ is the specific heat capacity of water, and M_{water} is

$$\frac{k_{eff}}{k_g} = 1 - \sqrt{1-\epsilon_b} + \frac{2\sqrt{1-\epsilon_b}}{1-\lambda B}\left(\frac{(1-\lambda)B}{(1-\lambda B)^2}\ln\frac{1}{\lambda B} - \left(\frac{B+1}{2}\right) - \left(\frac{B-1}{1-\lambda B}\right)\right) \quad (11)$$

the molar mass of the water.

The effective thermal conductivity, k_{eff}, can be estimated using Zehner and Schlunder model.

$$B = 1.25\frac{(1-\epsilon_b)^{10/9}}{\epsilon_b} \quad (12)$$

where, k_g is the thermal conductivity of the gas, $\lambda = \frac{k_g}{k_p}$, k_p is the thermal conductivity of the salt, and the term B is the shape factor given by the following equation:

$$A_{wall}\rho_{wall}C_{p,wall}\frac{\partial T_{wall}}{\partial t} = \pi d_i h_i (T - T_{wall}) - \pi d_o h_o (T_{wall} - T_a) \quad (13)$$

Reactor wall heat balance

In the above equation, the final term represents the heat loss from the packed bed to the reactor wall. It contains the term T_{wall} which is to be obtained from heat balance of the reactor wall.

where, A_{wall} is the cross sectional area of the wall, ρ_{wall} is the density of the wall, $C_{p,wall}$ is the specific heat capacity of the wall, d_o is the outer diameter of the reactor vessel, h_o is the heat transfer coefficient of the wall to the atmosphere and T_a is the ambient temperature.

$$Nu_o = \left(2 + \frac{0.387Ra^{1/6}}{(1+(0.492/Pr)^{9/16})^{8/27}}\right)^2 \quad (14)$$

Heat is removed from the outer surface by natural convection and the value of the external heat transfer coefficient is obtained from the Nusselt number at the outside wall of the reactor [17].

where, *Ra* is the Rayleigh number and *Pr* is the Prandtl number.

The heat transfer coefficient at the inside surface of a porous bed can be estimated using Leva's correlation [20].

1.1.1 Darcy's law

The governing equations described above require the velocity field. There are many empirical relations available

$$u = -\frac{K}{\mu}\Delta p \quad (15)$$

for the velocity field in a porous medium. In this analysis Darcy's law is used.

Darcy's law relates the pressure drop (head) to the flow rate across a porous column. The velocity 'u' can be expressed as: where, Δp is the pressure drop across the reactor and K is the permeability of the porous medium, where K is a function of porosity and particle diameter as given by the expression below:

$$K = \frac{\epsilon_b d_p^2}{180(1-\epsilon_b)^2} \quad (16)$$

These governing equations are being non-dimensionalised and then discretized using finite volume method and solved. The reactor wall heat balance equation is discretized using FDM method since there is no requirement of spatial discretization.

The various parameters affecting the performance of the system are pressure drop across the reactor (Δp), particle diameter of the salt (d_p), water vapour concentration at inlet (c), porosity of the packed bed (ϵ_b), and thermal mass of the reactor wall ($\rho_{wall}C_{p,wall}$).

Grid independence and validation

A grid independence study is preformed to model the domain, Fig 2 shows the non dimensional temperature change as a function of non dimensional time at varying grid sizes at z = 0.5, ϵ_b = 0.7, Δp = 0.4, d_p = 35μm, c = 0.6 mol/m^3 and $\rho_{wall}C_{p,wall}$ = 10000. Where 'z' is the position (centre of the reactor).

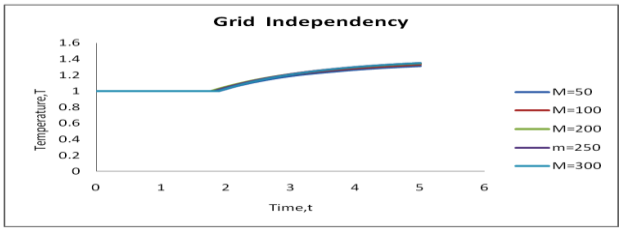

Fig 2. Grid Independency Test

The analysis is done for 5 different grid sizes with the number of grid points M = 50, 100, 200, 250, and 300. It is evident from Fig 2 that the results become grid independent at

M=250. The variation of temperature between grid point M=250 and M=300 is less than 1% (Table 1).In order to validate the model, the results thus obtained were compared with the experimental data (shown in Fig 3) for hydration of Zeolite 13 X reported by Gaeini et al. [17]. Fig 3 shows the transient variation of temperature at different positions of the reactor.

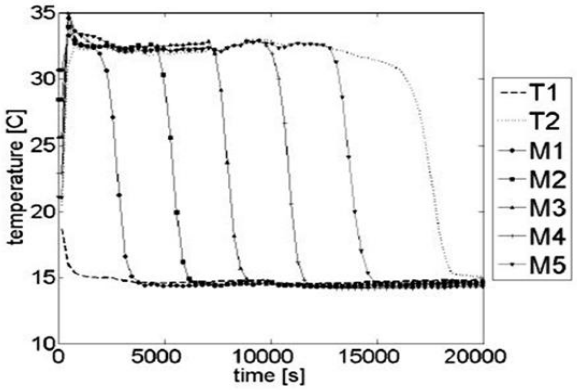

Fig 3. Temperature vs. time for different positions Gaeini et al. [17]

The reactor used in the work by Gaeini et al [17] was of 0.1 m length. M1 in Fig 3 represents the temperature at 0.025 m. It reaches to a value of almost 35 ^{o}C at a time of about 1000 s. This value is compared with the result (Fig 4) obtained from the present model with the same working material and working conditions as in the case of Gaeini et al. Fig 4 shows the variation in non-dimensional temperature as a function of non-dimensional time, varying from time t=0 to 10000. The non dimensional temperature reaches a maximum of 1.027 at about t=1000. The equivalent value of maximum temperature obtained by multiplying the reference value of temperature (300 K) is 308.1 K (35.1 ^{o}C) and the time is 1000 s. These results are same as the result from Gaeini et al [17], thereby the model is validated.

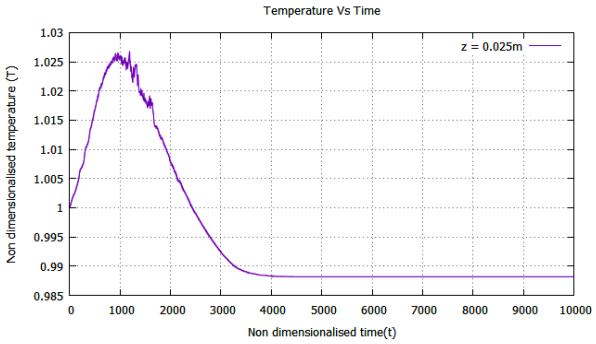

Fig 4. Non dimensional Temperature vs. Non dimensional time for validation

III. RESULT AND DISCUSSION

The modeling of the domain is carried out with grid size 250 and with the following boundary conditions porosity = 0.75, pressure drop = 0.3 bar, particle diameter=35 µm, inlet water vapor concentration = 0.9 mol/m^3 and wall heat capacity = 26720 J/ m^{3}K. The results of the modeling are presented in this section. Fig.5 shows the variation of temperature with time at various axial positions, z = 0.25, 0.5, 0.75, 1.

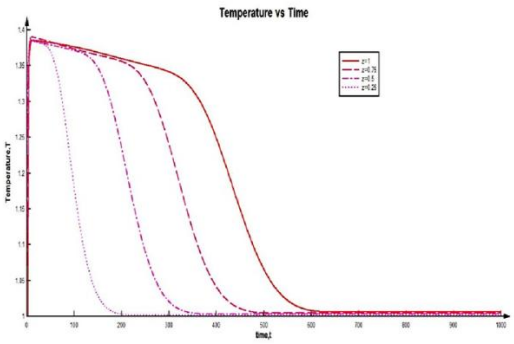

Fig 5. Axial distribution of Non Dimensional Temperature

For z = 1, the temperature remains at T = 1 up to t = 0.255, then suddenly increases up to a maximum value of T = 1.38 following which it linearly decreases up to t = 350. It then decreases suddenly up to t = 550 after which it decreases asymptotically and reach the initial value at t = 624. The temperatures at other points also follow similar pattern. The rate of increase is maximum for z = 0.25 compared to the other positions. This happens because thermo-chemical reaction starts only when the water vapor is available at the inlet. Since the adsorption process is exothermic, the enthalpy of adsorption gets liberated as heat and during this process water vapor gets adsorbed. So, the salt particles nearer to the inlet get into contact with the water vapor early than the particles at locations away from the inlet. The temperature starts to decrease due to heat losses through the reactor wall to the surrounding. As the moist air entering from the inlet is at ambient temperature, it also absorbs heat and the overall temperature decreases.

As the moist air flows through the porous medium, the vapor is adsorbed by the salt particles. Therefore, the air at the exit of the reactor will be mostly dry. This is evident from vapor concentration c = 0 up to t = 10 at the outlet (Fig 6). After t = 10, the vapor concentration increases and reaches the value equal to the inlet condition and remains constant. This is because the adsorption process is completed all along the reactor, and no more vapor adsorption is possible in the reactor.

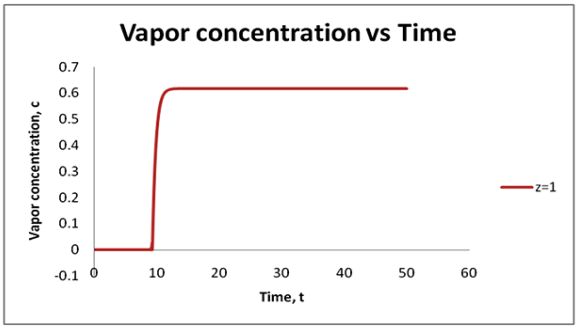

Fig 6. Non Dimensional Vapor concentration vs. Non dimensional time at outlet

A. *Optimisation of parameters using Thaguchi Method*

Taguchi suggested the use of orthogonal arrays instead of a full factorial design for designing the experiments. According to the Thaguchi

method optimization of the factors are done by a 4 level 5 factor orthogonal array. 16 different simulations were conducted up to time t = 1000. Three different responses were recorded and the results are obtained.

The three different time responses are:

- Beginning of the temperature rise of the air at the outlet of the reactor.
- Air temperature attaining at the outlet, and
- Heat carried away by the air at the outlet.

$$Q = \rho_g C_{p,g} \frac{\pi d_i^2}{4} u \int \Delta T dt \quad (17)$$

This can be obtained from the integration of the ΔT vs t curve.

Effect of porosity

Porosity is the ratio of the void space to the total space in the domain. More porous the medium, lesser the amount of salt in the domain and faster the flow of moist air through the medium. Fig.7 shows the effect porosity on time required to start the reaction and its effect on the rise in the outlet temperature, the effects of porosity on the maximum temperature attained at the outlet is also shown in Fig.7. Fig. 8 shows the heat liberated by the salt material during the reacton. It can be seen that as the porosity increases the time required to attain temperature rise decreases. This is due to the fact that the velocity of flow is higher when the porosity is high, which leads to a faster rate of adsorption and heat release. The maximum temperature attained at the outlet of the domain decreases as the porosity increases. This can be attributed to the higher velocity of flow, leading to lower residence time. But the heat liberated during the time interval t = 0 to t = 1000 in the form of sensible heating of the outlet air, increases with the porosity.

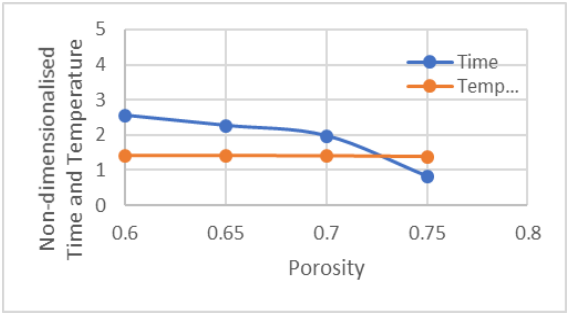

Fig 7. Effect of porosity on reaction time and temperature.

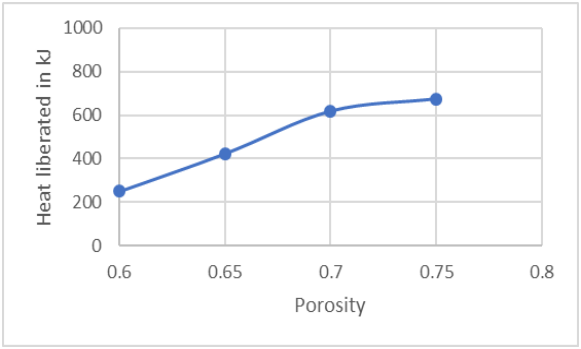

Fig 8. Effect of porosity on heat liberated.

Pressure drop across the reactor

The effect of fluid pressure drop across the domain is similar to that of porosity. As shown in Fig. 9 as the velocity of flow increases the pressure drop also increases along with increased rate of convection of vapor and heat. The temperature increases at outlet at lesser rate. The maximum temperature obtained at the outlet decreases with increase in pressure drop across the reactor. This is due to the lesser residence time of contact between the vapor and salt particles. The heat liberated increases as the pressure drop increases shown in fig. 10 because, the sensible heating of the outlet air increases with increased flow rate of the moist air.

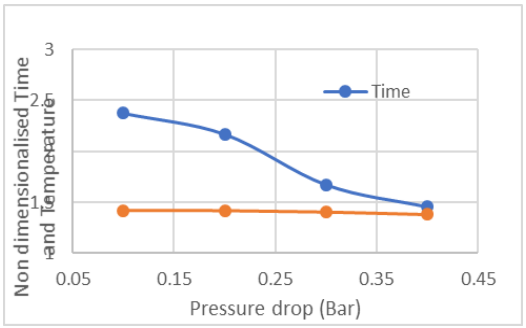

Fig 9. Non-dimensional time and Temperature as a function of pressure drop

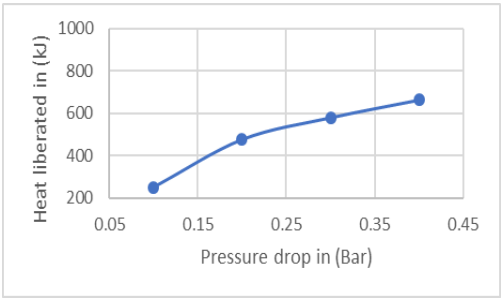

Fig 10. Heat liberated Vs Pressure drop

Particle diameter

Particle diameter plays an important role in the reaction kinetics of the adsorption process. Finer the particle size, higher is the mass transfer coefficient of adsorption process. Less resistance for adsorption leads to more heat release. So coarser the particle size, more time is required for the temperature to rise in the outlet as shown in Fig 11. The maximum temperature is higher in the case of finer particles due to the improved adsorption characteristics. But the total heat liberated is found increasing with increasing particles size Fig. 12.

This is because increasing the particle size increases the permeability of the porous medium.

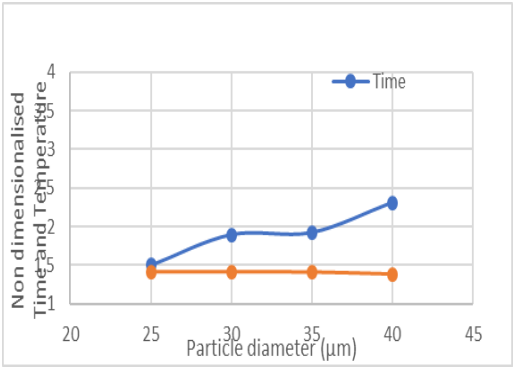

Fig. 11. Non-dimensional time, Max Non-Dimensional Temperature as a function of Particle Diameter (µm)

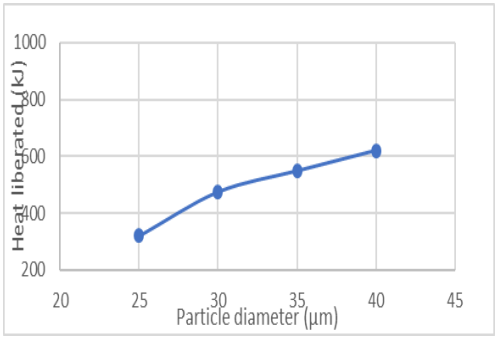

Fig. 12. Heat liberated in kJ as a function of particle diameter

Water vapour concentration

The effect of inlet water vapor concentration on time required to start the rise in the outlet air temperature is shown in Fig. 13. As the concentration of water vapor at the inlet region is high the vapor gets convected downstream and reaction rate increases. Fig 13 shows that the maximum temperature attained decreases when the inlet vapor concentration is increased. The heat liberated from the thermo-chemical material decreases with increase in inlet vapour concentration and is shown in Fig.14

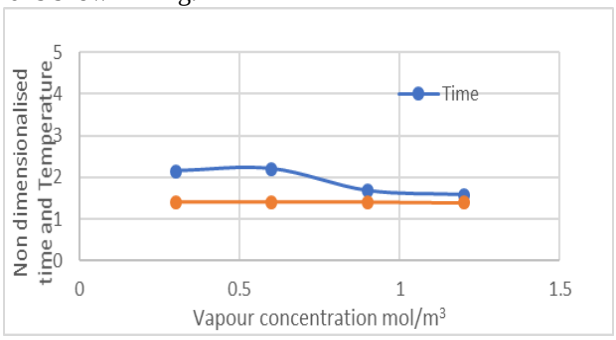

Fig 13. Non-dimensional time, Max Non-Dimensional and Temperature as a function of Inlet Vapor Concentration (mol/m^3)

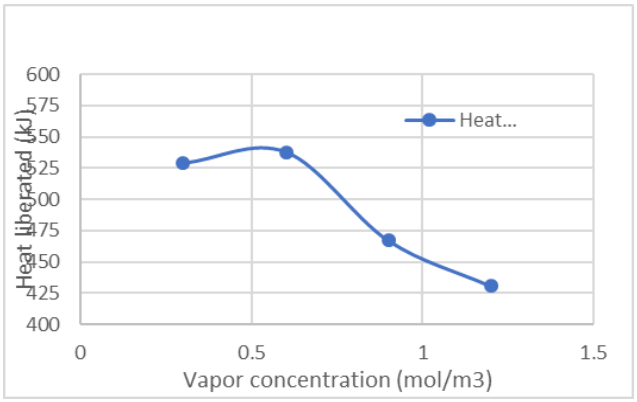

Fig 14. Heat liberated as a function of vapour concentration

Volumetric heat capacity

The volumetric heat capacity of the wall which is enclosing the thermo-chemical material ($\rho_{wall}\, C_{p,wall}$) signifies the ability of the reactor wall to conduct heat from the porous medium to the external surrounding. If the volumetric heat capacity is high, the rise in the wall temperature shall be negligible. Thus, the temperature difference between the bed and the reactor wall will be larger, owing to higher heat loss. Fig 15 shows the effect of volumetric heat capacity on time required to start the rise in the outlet air temperature and maximum temperature attained at the outlet. There is not much effect in the time required for the onset of temperature rise with increasing heat capacity. The maximum temperature decreases as the heat capacity increase because of the increase in the heat loss through the reactor wall. The heat liberated shows a similar behavior. Heat liberated shows a minor decrease with increase in heat capacity Fig. 16.

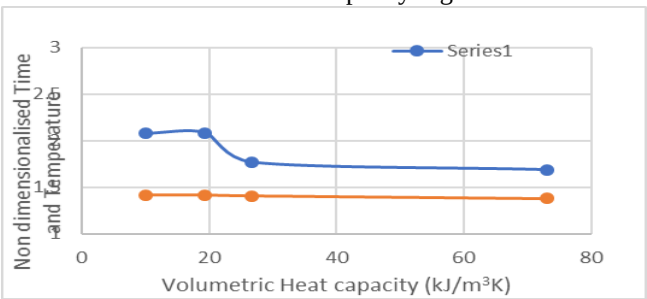

Fig 15. Non-dimensional time, Max Non-Dimensional Temperature as a function of Volumetric Heat Capacity of Wall

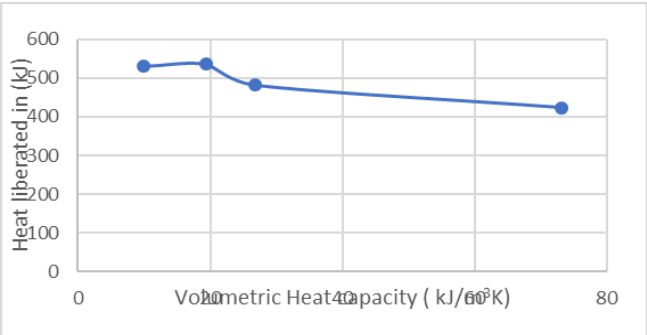

Fig 16. Heat liberated Vs. Volumetric heat capacity

IV. CONCLUSION

Modeling of energy release from a fixed bed filled with $MgSO_4$ on hydration using the finite volume method shows the effect of various design and operating parameters on the performance of the bed. The porosity of the bed plays an important role in determining the velocity of flow in the medium along with the pressure drop. Since the void space between the particles increases with porosity, the temperature of the outlet air increases at a higher rate. But the maximum temperature attained for the same flow rate is found to decrease when both porosity and pressure drop increase, because of less residence time of the air. The particle diameter plays an important role on adsorption kinetics. Finer the particle size, larger is the mass transfer coefficient. Another important factor which affect the performance of the reactor is the vapor concentration of the inlet air. Higher the vapor concentration of supply moist air, faster is the reaction rate and lesser the time required to attain the maximum temperature. Thus, while designing a thermochemical reactor, the porosity of the reactor, mass flow rate of moist air, particle diameter of the salt, and vapor concentration of the inlet moist air are to be optimized to get the maximum performance from the reactor bed.

The charging temperature of the $MgSO_4$ salt can be easily attainable with a solar collector, so we can integrate the thermochemical reactor with a solar charging system or a waste heat recovery system. Main applications of this energy storage system are domestic hot water supply, drying process, seasonal storage of thermal energy etc. Main drawback of this system is the sudden release of the heat when it is in contact with the water vapour. Controlling the chemical reaction is very difficult once it is initiated. This can be done by controlling the vapour content or humidity of the air passing through the reactor bed. But more in-depth studies are required in this area.

REFERENCES

1. A.H. Abedin, M.A. Rosen, A Critical Review of Thermochemical Energy Storage Systems, Open Renew. Energy. J. 4(2011)42–46. DOI:10.2174/1876387101004010042
2. J. Cot-Gores, A. Castell, L.F. Cabeza, Thermochemical energy storage and conversion: A-state-of-the-art review of the experimental research under practical conditions, Renew. Sust. Energ. Rev. 16 (2012) 5207-5224. DOI: 10.1016/j.rser.2012.04.007.
3. K. Darkwa, P.W. O'Callaghan, Green transport technology (GTT): Analytical studies of a thermochemical store for minimising energy consumption and air pollution from automobile engines, Appl. Therm. Eng. 17 (1997) 603-614. DOI: 10.1016/S1359-4311(97)80001-4.
4. H. Druck, B. Mette, H. Kerskes, Concepts of long term thermochemical energy storage for solar thermal applications- selected examples, Energy Procedia. 30 (2012) 321-330. DOI: 10.1016/j.egypro.2012.11.038
5. A. Solé, X. Fontanet, C. Barreneche, A.I. Fernández, I. Martorell, L.F. Cabeza, Requirements to consider when choosing a thermochemical material for solar energy storage, Solar Energy. 97 (2013) 398-404.
6. D. Aydin, S.P. Casey, S. Riffat, The latest advancements on thermochemical heat storage systems, Renew. Sust. Energ. Rev. 41 (2015) 356-367. DOI: 10.1016/j.rser.2014.08.054.
7. A. Agarwal, R.M. Sarviya, An experimental investigation of shell and tube latent heat storage for solar dryer using paraffin wax as heat storage material, JESTECH. 19 (2016) 619-631. DOI: 10.1016/j.jestch.2015.09.014.
8. Y.I. Aristov, D.M. Chalaev, B. Dawoud, L.I. Heifets, O.S. Popel, G. Restuccia, Simulation and design of a solar driven thermochemical refrigerator using new chemisorbents, Chem. Eng. J. 134 (2007) 58-65. DOI: 10.1016/j.cej.2007.03.070.
9. G. Balasubramanian, M. Ghommem, M.R. Hajj, W.P. Wong, J.A. Tomlin, I.K. Puri, Modeling of thermochemical energy storage by salt hydrates, Int. J. Heat Mass Transf. 53 (2010) 5700-5706. DOI: 10.1016/j.ijheatmasstransfer.2010.08.012.
10. M. Ghommem, G. Balasubramanian, M.R. Hajj, W.P. Wong, J.A. Tomlin, I.K. Puri, Release of stored thermo- chemical energy from dehydrated salt, Int. J. Heat Mass Transf. 54 (2011) 4856-4863. DOI: 10.1016/j.ijheatmasstransfer.2011.06.041.
11. M.N. Azpiazu, J.M. Morquillas, A. Vazquez, Heat recovery from a thermal energy storage based on the Ca(OH)2/CaO cycle, Appl. Therm. Eng. 23 (2003) 733-741. DOI:10.1016/S1359-4311(03)00015-2.
12. F. Bertsch, B. Mette, S. Asenbeck, H. Kerskes, H. Müller-Steinhagen, Low temperature chemical heat storage - an investigation of hydration reactions. Technical report, Institute for Technical Thermodynamics, German Aerospace Centre. (2009).
13. H.A. Zondag, M. Van essen, L.P.J. Bleijendaal, B. Kikkert, M. Bakker. Application of $MgCl_2{\cdot}6H_2O$ for thermochemical seasonal solar heat storage, 5th International Renewable Energy Storage Conference, 2010.
14. A.H. Abedin, M.A. Rosen, Assessment of a closed thermochemical energy storage using energy and exergy methods, Appl. Energy. 93 (2012) 18-23. DOI: 10.1016/j.apenergy.2011.05.041.
15. D. Stitou, N. Mazet, S. Mauran, Experimental investigation of a solid/gas thermochemical storage process for solar air-conditioning, Energy. 41 (2012) 261-270. DOI: 10.1016/j.energy.2011.07.029.
16. V.M. van Essen, H.A. Zondag, J. Cot Gores, L.P.J. Bleijendaal, M. Bakker, R. Schuitema, W. van Helden, Z. He, C.C.M. Rindt, Characterization of MgSO4 Hydrate for Thermochemical Seasonal Heat Storage, J. Sol. Energy Eng. 131(2009), 041014. DOI:10.1115/1.4000275.
17. M.Gaeini, H.A. Zondag, C.C.M. Rindt, Non-isothermal kinetics of zeolite water vapor adsorption into a packed bed lab scale thermochemical reactor, International Heat Transfer Conference, 2014. Proceedings of the IHTC-15, IHTC15-9169-1/11.
18. D.C. Montgomery, Design and Analysis of Experiments, eighth ed., Wiley, United States, 2013.
19. W. John Thomas, Barry Crittenden, *Adsorption Technology and Design*, 1998, Elsevier Science & Technology Books.
20. Leva, M., "Fluid flow through packed beds," Chemical Engineering Science, 56(115), (1949).
21. N. *Wakao* and T. *Funazkri*, "Effect of Fluid Dispersion Coefficients on Particle-To-Fluid Mass Transfer Coefficients in Packed Beds Correlation of Sherwood Numbers," Chemical Engineering Science, Vol. 33, No. 10, 1978, pp. 1375-1384.